Int. J. Electrochem. Sci., 14 **(2019)** 8173 – 8184, doi: 10.20964/2019.08.84

International Journal of
ELECTROCHEMICAL
SCIENCE
www.electrochemsci.org

Investigation of Corrosion Resistance of poly(o-phenylenediamine)-ZnO Composites on Stainless Steel

Chaogang Zhou[1], *Chaojin Zhou*[2], *Jiawei Zhang*[3,*]

[1] College of Metallurgy and Energy, Key Laboratory of the Ministry of Education for Modern Metallurgy Technology, North China University of Science and Technology, Tangshan 063009, China
[2] School of Materials Science and Engineering, Guangdong Provincial Key Laboratory of Advanced Energy Storage Materials, South China University of Technology, Guangzhou 510641, China
[3] School of Metallurgy, Northeastern University, Shenyang 110819, China
[*]E-mail: zhang416940558@163.com

Received: 31 March 2019 / *Accepted:* 20 May 2019 / *Published:* 30 June 2019

The poly(o-phenylenediamine)-ZnO (PoPD-ZnO) composite were synthesized by in-situ polymerization, and the waterborne polyurethane was used as the binder. The corrosion inhibition performance of the PoPD-ZnO composite coating on stainless steel was investigated. The structures of homopolymer PoPD and PoPD-ZnO composite were characterized by Fourier transform infrared spectroscopy (FTIR), X-ray diffraction (XRD) and scanning electron microscopy (SEM). Cyclic voltammetry demonstrates the redox properties and stability of the composite. After soaking in 3.5% NaCl for a certain period of time, the corrosion resistance of the polymer coating was studied by potentiodynamic polarization and electrochemical impedance spectroscopy (EIS). The results show that the homopolymer PoPD coating and the PoPD-ZnO composite coating can protect the stainless steel. The corrosion rate of the PoPD-ZnO composite coating with good corrosion resistance is 1.9% of bare steel. In addition, the addition of nano-ZnO facilitates the formation of a compact and low-defect coating, thereby impeding the erosion of corrosive media and improving the corrosion resistance of PoPD coatings.

Keywords: poly(o-phenylenediamine) (PoPD); ZnO; Steel; polymer coating; anticorrosion

1. INTRODUCTION

Conductive polymers (CPs) have been studied for the replacement of inorganic electrons, optoelectronics, and semiconductor materials due to their mechanical strength, electrical conductivity, corrosion stability and possibility of both chemical and electrochemical synthesis [1,3]. The benzene ring and the π bond are usually present in the polymer, which facilitates electron transport of the polymer and the external environment, thereby make them useful in wide area of applications. The charge is located on the area of several repeating units such as benzene ring and the π bond, which is

considered as a charge carrier in conductive polymers. The repeating units facilitate local charges move along the polymer chain, and thereby make them useful in the wide area of applications. [4] At this background, (poly-aniline) (PANI) and its derivatives (such as polypyrrole and polythiophene) attract much research interest due to advantages like easy synthesizability, architecture flexibility, environmental stability, non-toxicity and high potential value. [5].

An important role in corrosion resistance is played by conductive polymers-inorganic oxide nanocomposites [6]. In the field of corrosion, the addition of organic nanoparticles facilitates the design of composite coatings with good inhibition. [7-11]. Since its environmental-friendly properties [12,13], low cost, excellent mechanical and chemical stability, nano-ZnO particles have caused widespread concern. Electron mobility is the reason why most polymers are restricted to conductors, but conductive polymers can be converted into semiconductor materials after introduction of doped acid. Doping acid into the polymer can form a hole conductor (p-type) material, and ZnO is a good electron acceptor (n-type), when they are mixed together, they form a p-n structure and greatly increase the electron transfer ability [14].

Although PANI exhibits good corrosion resistance, the poor processability of PANI powder and the low adhesion to metal substrates severely limit its application. PoPD is a derivative of PANI, and its introduction of electron donating group significantly improve the physical properties and corrosion resistance of PANI [15]. PoPD is very stable in acid, neutral, and alkaline solutions and air and can prepare in above aqueous [16]. It has apparently different molecular structure when compared with PANI. Unlike the parent polymer polyaniline which has a linear structure, PoPD is a ladder-type polymer.[17] It has been reported that there existence a highly aromatic hydrocarbon polymer containing repeating units of 2,3-diaminophenazine or quinoxaline [18,19]. Additionally, the electrochemical and physical properties of PoPD differ significantly from polyaniline. When the potential is increased to +1 V, PoPD is less prone to electrochemical degradation, while polyaniline is not. Compared with PANI, PoPD has extremely high thermal stability and strong adsorption [18-21].

Luis has been electrosynthesized PoPD films on 304 stainless steel in aqueous solution of phosphoric acid. They noted that the reduced form of PoPD in a translucent green state provides a fairly good protection against pitting for steel in highly aggressive chloride medium [22]. Aboozar founded that compared with pure polyester coating, the nanocomposite coatings have fewer pores and better inhibit the penetration of erosive ions. While preventing the corrosion particles from diffusing near the metal, the nano-inorganic particles ZnO fill the pores of the polymer, thereby enhancing the effect of the corrosion inhibitor of the coating.[23,24].

To the best of our knowledge, few literature on the coating of poly(o-phenylenediamine)-ZnO composite has been published as corrosion protection for steel in chloride media. In this paper, we used stainless steel as the substrate, and prepare poly(o-phenylenediamine) and poly(o-phenylenediamine)-ZnO by chemical oxidation. The reversibility and stability of poly(o-phenylenediamine) and poly(o-phenylenediamine)-ZnO were investigated by cyclic voltammetry. The corrosion resistance of poly(o-phenylenediamine) coating and poly(o-phenylenediamine)-ZnO composite coating on stainless steel samples was studied at room temperature in 3.5% NaCl.

2. EXPERIMENTAL

2.1 Materials

o-Phenylenediamine (oPD), ammonium persulfate (APS), butanol, dibutyl phthalate, ethyl acetate, N-methyl-2-pyrrolidone (NMP), NaCl are analytical grade and were available for immediate use. ZnO (99.9 %, 30 ± 10 nm) was obtained from Shanghai Aladdin Biochemical Technology Co., Ltd. Waterborne polyurethane (WPU) purchased from Jiaxing Dongjing Printing and Dyeing Material Co., Ltd. The steel specimens of dimension 20 × 20 × 1.1 mm were mechanically polished with SiC papers (according to the sequence of 320, 600, 1000 grade). After washing and degreasing with acetone and distilled water, it was dried in the air.

2.2 Synthesis of poly(o-Phenylenediamine)-ZnO powders

poly(o-Phenylenediamine) (PoPD) and poly(o-Phenylenediamine)-ZnO (PoPD-ZnO) were synthesized by in situ emulsion polymerization method, and a given amount of HCl and monomers were mixed according to the molar ratio of 1:1. The typical chemical oxidative polymerization process of PoPD is as follow: 5.4 g of o-Phenylenediamine was added into 50 ml of 1 M HCl under a series of ultrasonic vibrating, magnetic and vigorous stirrings, and then 50 mL of 1 M APS solution was added dropwise into the above solution. The resulting mixture was allowed to react for 20 hrs below 5 °C. After that, the precipitate was filtered and washed using double distilled water and ethanol to remove extra acid and oxidant until the filtrate into colorless, and then moved them in the vacuum oven to dry at 60°C for 24hrs. The PoPD product will be ground and ready for use. After adding 0.25 g of nanoparticle ZnO to a three-necked flask, the above synthetic copolymer step was repeated to obtain a composite material. [25].

2.3 Preparation of poly(o-Phenylenediamine)-ZnO composite coatings

The anticorrosion coating was prepared by 0.2 g of PoPD-ZnO was dissolved in 0.4 ml of NMP and 0.2 ml of ethyl acetate. After thorough mixing, 1 g of WPU binder was added to each solution by sonication. After obtaining a uniform solution of a certain viscosity, the solution is applied flat on the pretreated substrate by the aid of a brush. The coating was allowed to stand dry overnight at room temperature, and then dried in a drying oven maintained at a temperature of 60 °C for 10 to 24 hours. After the coating was cured, the thickness of all coating films was measured using an AIRAJ micrometer to a range of 480 ± 3 μm. The PoPD coating without composite ZnO follows the above preparation process. Figure 1 shows the schematic diagram preparation of poly(o-phenylenediamine)-ZnO coatings onto the stainless steel substrate.

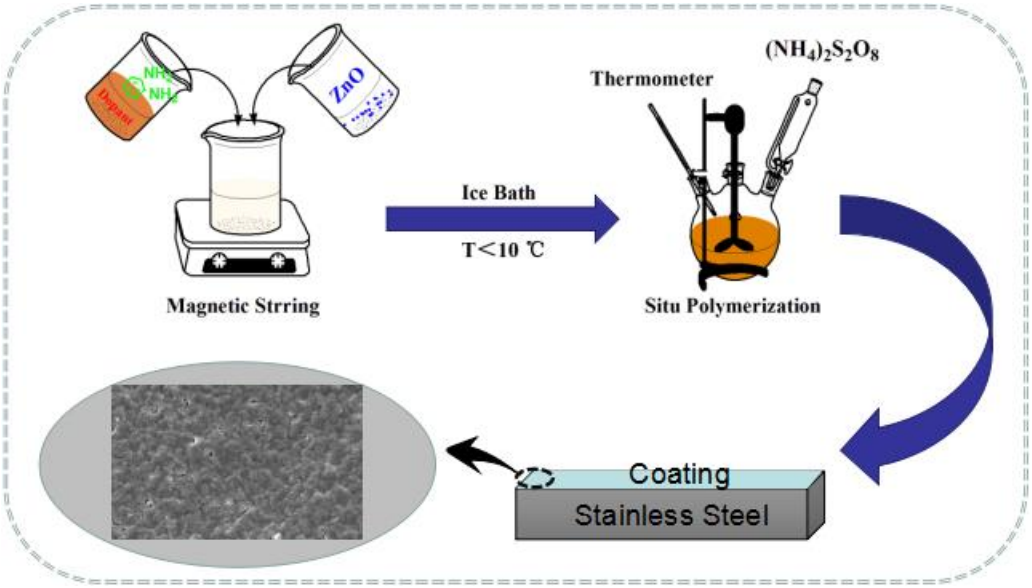

Figure 1. The schematic diagram preparation of poly(o-phenylenediamine)-ZnO coatings.

2.4 Characterization

The chemical structure of the sample was studied by Fourier transform infrared spectroscopy (FTIR, Nicolet 6700), and the characterization range was from 4000 to 500 cm^{-1}. The crystal form of the sample was determined in an X-ray diffraction (XRD, Smart Lab X) with a working range of 10 to 90° (λ = 0.15406 nm), Cu K-alpha radiation, and 45 kV/200 mA. The morphology of the homopolymer and copolymer nanocomposites and the corresponding coatings was examined by a field emission scanning electron microscope (FESEM, ZEISS Supera 55) with an accelerating voltage of 5 kV. Potentiodynamic polarization and electrochemical impedance spectroscopy (EIS) measurements were carried out with CHI660E electrochemical workstation at room temperature. Potentiodynamic polarization curves were measured at open circuit potential ± 250 mV(vs. SCE) with a constant scan rate of 1 mV/s, and the EIS curves were performed by utilizing a sine wave with 0.005 V amplitude under the frequency range of 10^5 Hz to 10^{-2} Hz, and the EIS data were analyzed by Zview software.The experiment was performed three times and the same trend of protection efficiency was obtained.

3. RESULTS AND DISCUSSION

3.1 Structures and morphology of poly(o-Phenylenediamine)-ZnO

The FTIR spectra and XRD patterns of PoPD and PoPD-ZnO are shown in (Figure 2). The polymerized PoPD in the presence and absence of ZnO was scraped off and FTIR spectra of the polymer powderswere recorded in (Figuer 2a). As shown in (Figuer 2a), the peaks at 1632 and 1530 cm^{-1} are attributed to the C=C stretching vibrations of quiniod (Q) and benzenoid (B) rings

respectively. The C-N stretching vibrations of quinoid and benzenoid rings are appearing at 1365 and 1247 cm^{-1} respectively [26]. The two peaks appeared at 3320 and 3153 cm^{-1} are ascribed to the stretching vibrations of –NH– and $–NH_2$ respectively [27,28]. The FTIR peaks of PoPD-ZnO are slightly shifted to higher or lower wavenumber, when compared to PoPD. This is attributed to the O-H bond and the N-H bond present in the nano-ZnO and PoPD chains, respectively, caused by the overlap of the stretching-related peaks.The absorption peak corresponding to ZnO (JPDS No. 36-1451). Appear in the PoPD-ZnO pattern, which indicates the successful loading of ZnO with PoPD polymers. [28].

The XRD patterns of PoPD and PoPD-ZnO are illustrated in (Figure 2b). The XRD patterns results show the sharp peak around at 2θ=10° to 30° .These sharp peaks are indicating the partial crystalline nature of PoPD. The broad peak centered at 2θ=26.4° reveal that the local crystallinity may be caused by the periodicity perpendicular to the polymer chain [26,28,29]. The partial crystallinity may also be resulted from the long range ordering of polymer chains and the doping of HCl. furthermore, Samanta indicates that the nature of the synthesized PoPD having well-alligned morphology was confirmed by the crystalline peaks located at 2θ = 10.7°, 16.6°, 18.4° and 28.8° [30]. In the XRD curve of PoPD-ZnO, the crystallization peaks at 2θ = 31.8°, 34.4°, 36.3°, 47.5° and 56.6° correspond to composite ZnO particles where is fully matching with JCPDS card No. 36-1451.

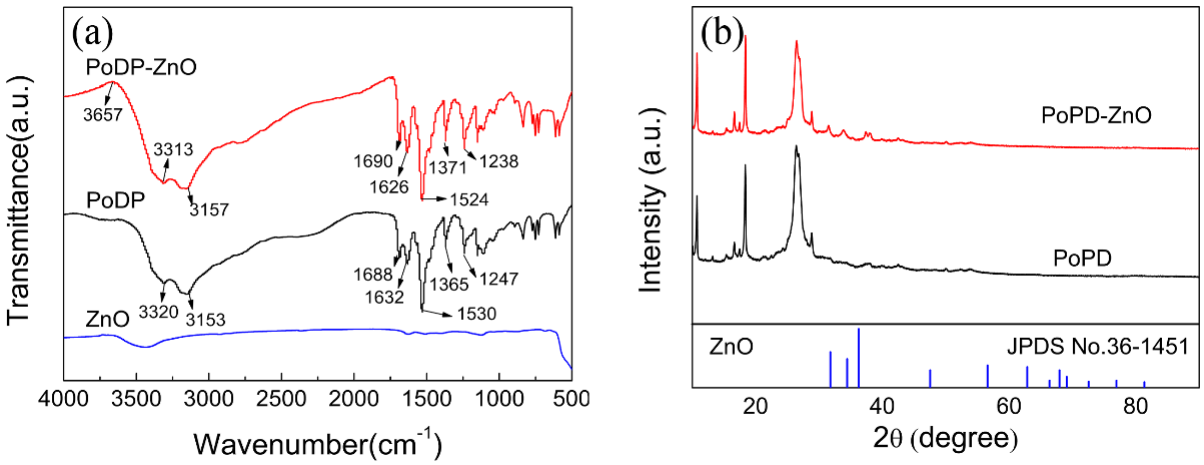

Figure 2. (a) FTIR spectra of PoPD and PoPD-ZnO; (b) XRD patternsStructure analysis of PoPD and PoPD-ZnO.

The surface morphologies of polymers were investigated by FESEM in (Figure 3). It can be seen from (Figure 3), the images of PoPD and PoPD-ZnO all show the aggregated structures. The PoPD exhibit a larger lumphy structure with the diameter range of 2-3 μm, and irregularly shaped sheets and granules attached to its surface. While PoPD-ZnO consists of a stack of stick-like structure that with a size of about 1μm and smooth surface. From the FESEM images of PoPD-ZnO, it is confirmed that the morphology of PoPD is affected by ZnO nanoparticles. Combining the above two graphics of FTIR and XRD indicateing that ZnO nanoparticles are embedded in PoPD.

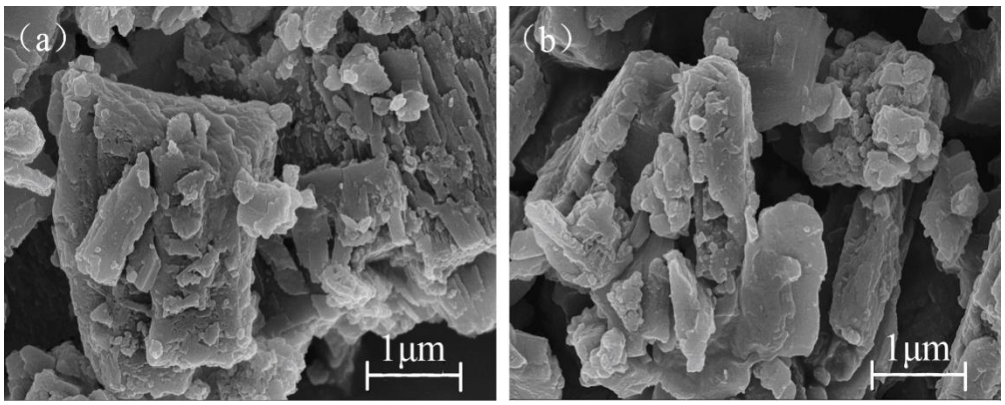

Figure 3. (a) Scanning electron micrograph of PoPD and (b) Scanning electron micrograph of PoPD-ZnO.

3.2 CV characterization of poly(o-Phenylenediamine)-ZnO Particles

The electrochemical activity and stability of PoPD and PoPD-ZnO were obtained by scanning the CV curves at a scan rate of 20 mVs^{-1} in 1.0 M HCl solution and are shown in (Figure 4). In the acidic solution, H^+ exists in the acidic solution to facilitate the reversible redox reaction of the polymer, and the parameters obtained are more obvious than other solutions. As shown in (Figure 4a), the CV curves of PoPD and PoPD-ZnO are display distinct redox peaks, which indicates all materials have reversible electrochemical activity and pseudocapacitive charge storage properties. The reversibility of the electrochemical redox reaction can be estimated by the potential ratio between the oxidation peak and the reduction peak, and the closer to 1, the higher the reversibility. From (Figure 4a), we can estimate that the oxidation potential and the reduction potential of the potential PoPD are about -0.097 V and -0.17 V, respectively, and the oxidation potential and the reduction potential of the PoPD-ZnO are about -0.1 V and -0.15 V, respectively.

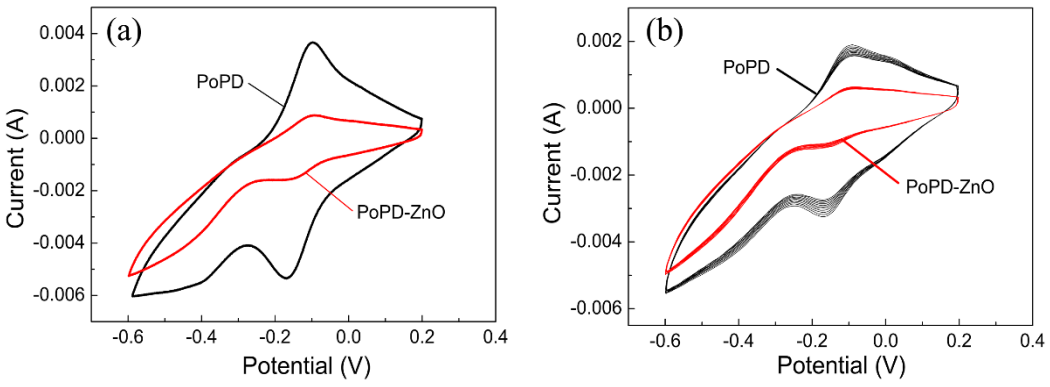

Figure 4. CV curves at a scan rate of 20 mVs^{-1} in 1.0 M HCl of PoPD and PoPD-ZnO (a) 1 cyclic voltammograms, (b) 20 cyclic voltammograms.

The redox current value of PoPD-ZnO is also about 2 times larger than PoPD. This may be because the introduction of ZnO nanoparticles does not change the electrochemical reversibility of PoPD, but it can exert a synergistic effect with PoPD, promote the redox reaction of PoPD chain, and

make the electrochemical behavior of PoPD-ZnO be better than PoPD. As shown in (Figure 4b), with the number of scan increasing, the current response decreased and the corresponding redox peak shapes broadened, indicating the good electrochemical stability of all the obtained materials.

3.3 Characterization of poly(o-Phenylenediamine)-ZnO composite coating surface morphology

Scanning electron microscopy (SEM) is extensively used in the surface analysis of synthesized materials. (Figure 5) demonstrates the SEM micrographs of the WPU coating (Figure 5a), PoPD coating (Figure 5b) and PoPD-ZnO composite coating (Figure 5c). As can be seen, there are some defects structures on the surfaces of the PoPD coating and PoPD-ZnO composite coating. This is due to the fact that residual soluble oligomers are soluble in the acid solution during doping. In addition, the presence of a doping medium affects the conductivity of the same type of polymer[26]. However, the porosity of the PoPD-ZnO composite coating is less than that of the PoPD coating, which is attributed to the fact that the polymer monomer can be effectively attached around the ZnO, increasing the degree of polymerization. On the other hand, ZnO can also be filled into the voids of the polymer, reducing the presence of voids.

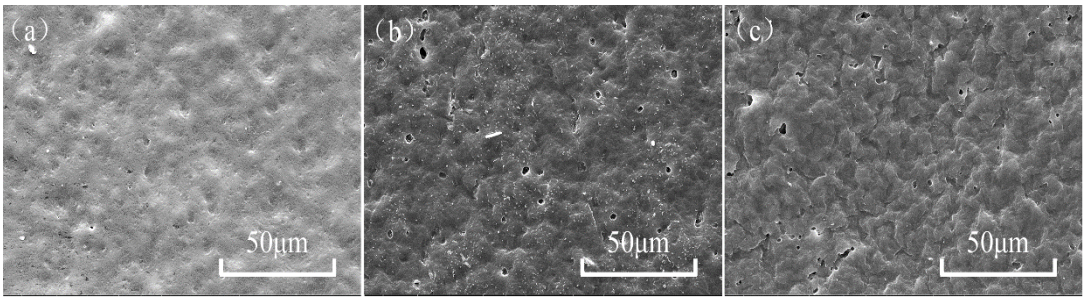

Figure 5. (a) Scanning electron micrograph of WPU coating, (b) Scanning electron micrograph of PoPD coating, (c) Scanning electron micrograph of PoPD-ZnO composite coating.

3.4 Corrosion protection evaluation of poly(o-Phenylenediamine)-ZnO Composite Coating

After immered the coating in a 3.5% NaCl solution for 168 h at room temperature, the corrosion resistance of the PoPD coating and PoPD-ZnO composite coating were evaluated by potentiodynamic polarization and EIS method and is shown in (Figure 6). Figure 6a shows the polarization curves of different coatings. The corrosion potential (E_{corr}) and the corrosion current density (I_{corr}) are obtained by extrapolation, and the corrosion rates (CR) of bare steel and different coatings are obtained by the following equations is also recorded in Table 1 [31].

$$CR = 3270 \times \frac{M(g) \cdot I_{corr}(A/cm^2)}{n \cdot \rho(g/cm^3)} \quad (1)$$

Where M is the molecular mass, it represents the molar mass of the working electrode metal. I_{corr} is corrosion current density, n is the number of electrons transferred by 1 mol of metal during the oxidation reaction, and ρ is the density of steel. As shown in (Figure 6a) and Table 1, also gives the corrosion parameters of WPU coating, PoPD coating and PoPD-ZnO composite coating calculated by equation (1). A negative shift in CR values of 3 and 6-fold have been found when PoPD and PoPD-

ZnO were applied to the WPU, respectively. Compared to uncoated steel, the E_{corr} of the coated sample moves in the positive direction and the I_{corr} moves in the negative direction, indicating that the coating acts as a barrier to the substrate and inhibits corrosion. The PoPD-ZnO composite coating has a higher E_{corr} and lower I_{corr}, which indicates that it has good corrosion resistance compared to WPU, and PoPD coating. This suggests that the addition of the PoPD-ZnO as a pigment of the WPU coating can effectively prevent further corrosion of the steel sample. The E_{corr} is increased from -0.82 V corresponding to coating free steel surface to -0.45 V after coated PoPD-ZnO composite film. Besides the I_{corr} values were found to decrease with coated WPU coating (3.06×10^{-5} A/cm^2), PoPD coating (1.23×10^{-5} A/cm^2) and the PoPD-ZnO composite coating (4.74×10^{-6} A/cm^2). The decrease in the I_{corr} indicates that PoPD-ZnO composite coating and PoPD coating can rely on the reversible redox properties of the polymer materials [32]. In the presence of ZnO nanocomposites, he corrosion resistance of the coating will also increase [33,34]. The results of potentiodynamic curves and EIS indicates that the PoPD and PoPD-ZnO inhibit the anodic reaction by acting as a barrier layer between electrode surface and corrosive environment [24,35]. The protection efficiency (PE%) of coatings was calculated by the following equation [36]:

$$PE(\%) = \frac{I_{corr} - I'_{corr}}{I_{corr}} \times 100 \quad (2)$$

where I_{corr} is the corrosion current density of steel and I'_{corr} is the corrosion current density of WPU coating, PoPD coating and PoPD-ZnO composite coating. Compared to bare steel, the protection efficiencies for WPU, PoPD and PoPD-ZnO coating estimated from the above equation are found to be 86.2%, 94.4% and 97.9%, respectively.

The corrosion resistances of the coated films was evaluated as electrochemical impedance, in 3.5% NaCl solution are presented in (Figure 6b). The resistances of the solution (R_s), the coating resistance (R_c) and the charge transfer resistance (R_{ct}) were fitted by the equivalent circuit inside (Figure 6b). The fitted images and data are shown in Figure 6b and Table 1, respectively. The corrosion process of the coating can be further understood by the shape of the Nyquist diagram. The corrosion mechanism controlled by the Nyquist diagram is semi-circular, while the diffusion control is linear.The semicircle in the Nyquist spectrum in (Figure 6b) indicates that the corrosion resistance mechanism of the coating is kinetically controlled. At the same time, a semicircle indicates the occurrence of a corrosion process , which includes the charge transfers resistance caused by metal corrosion and the double layer capacitance of the liquid/metal interface. In the Nyquist diagram, the high frequency region corresponds to the film impedance and the low frequency region represents the charge transfer impedance. The protection efficiencies (PE%) of the charge transfer resistance in Table 1 were calculated by the expression below [29,34]:

$$PE(\%) = \frac{R_{ct} - R^0_{ct}}{R_{ct}} \times 100\% \quad (3)$$

Where R_{ct} and R^0_{ct} are the charge transfer resistances of the coated steel and pristine steel, respectively. The value of R_c increased from 229.2 Ω·cm^2 for the WPU film to 259.6 Ω·cm^2 and 914.9 Ω·cm^2 upon the addition of PoPD film and PoPD-ZnO film, respectively. Furthermore, the R_ct of WPU, PoPD film and PoPD-ZnO film are 857.2 Ω·cm^2, 928.8 Ω·cm^2 and 1325 Ω·cm^2 resulting in 54.1, 57.6 and 70.3 % protection efficiency, respectively. Among them, the effect of PoPD-ZnO film was most

prominent, due to the introduction of ZnO nanoparticles in the polymer matrix resulting in an increase in the surface area of the coating, thereby increasing the charge transfer resistance of the electrode system. Generally, a large surface area facilitates contact of the composite coating with the corrosive medium, thereby improving the corrosion resistance of the coating. This is due to the special nature of the ionic interactions that the polymer can release in the corrosion reaction with steel in the presence of Cl^- ions [37].

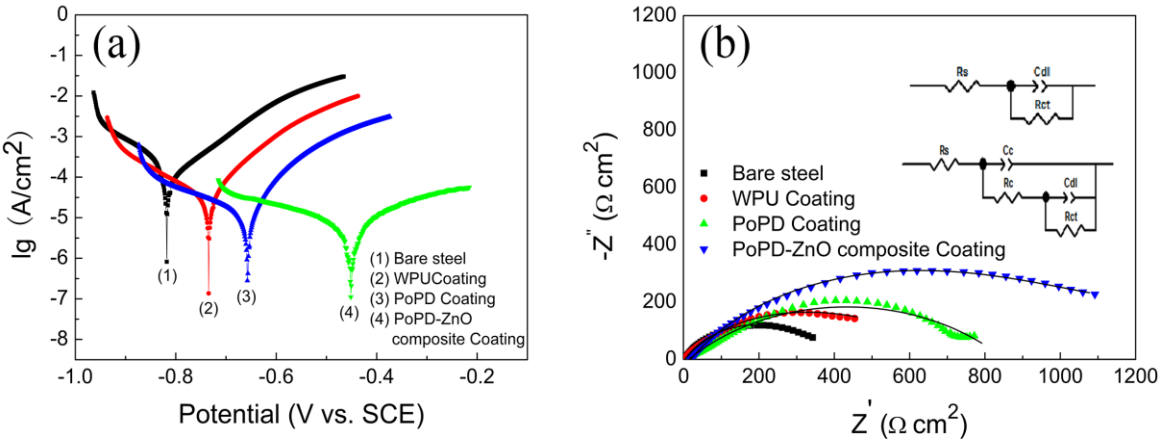

Figure 6. Corrosion protection evaluation curve of bare steel, WPU coating, PoPD coating and PoPD-ZnO composite coating immersed in 3.5% NaCl solution for 168 hours. (a) potentiodynamic polarization polts are perform at a scan rate of 1 mV/s at an open circuit potential of ±250 mV (vs.SCE) and (b) Nyquist plots were performed by 0.005 V amplitude under the frequency range of 10^5 Hz to 10^{-2} Hz, and the EIS data are analyz and fit by Zview software.

Table 1. Fitting corrosion parameters for bare steel, WPU coating, PoPD coating and PoPD-ZnO composite coating immersed in 3.5% NaCl solution for 168 hours by potentiodynamic polarization and EIS methods.

Coating	Potentiodynamic polarization				Impedance parameter values				
	E_{corr} (V)	I_{corr} (A/cm^2)	*C*R (mm/year)	*PE* (%)	R_s (Ω·cm^2)	R_c (Ω·cm^2)	R_{ct} (Ω·cm^2)	*PE* (%)	*chi-square*
Bare steel	-0.82	2.22×10^{-4}	2.57	—	3.4	—	393.5	—	
WPU	-0.74	3.06×10^{-5}	0.35	86.2	2.83	229.2	857.2	54.1	0.008
PoPD	-0.65	1.23×10^{-5}	0.41	94.4	13.8	259.6	928.8	57.6	0.012
PoPD-ZnO	-0.45	4.74×10^{-6}	0.05	97.9	18.8	914.9	1325	70.3	0.003

The potentiodynamic polarization and EIS electrochemical data shows that the PoPD-ZnO composite coating provides the highest corrosion protection for metal substrates. To confirm this result more intuitively, the corrosion pattern of the steel surface after 30 days of coating removal was observed (Figure 7). According to (Figure 7), it can be seen that the degree of corrosion of the steel surface after removal of the coating meets the following trends: bare steel > WPU coating > PoPD coating > PoPD-ZnO composite coating. As shown in the internal image of (Figure 7a), the metal surface is severely damaged, a large number of corrosion pits can be found, and corrosion products are distributed near the corrosion sites. From (Figure 7b,), (Figure 7c), (Figure 7d), it can be observed that

many corrosive white spots can be observed, and the number of spots in the steel surface under the PoPD coating is much larger than the steel surface under the WPU coating and the PoPD-ZnO composite coating. The area of each corrosion spot is again the largest under the PoPD coating coating. However, after removed the PoPD-ZnO composite coating, it can be seen from (Figure 7d) that the steel surface is covered with less amount of corrosion products and corrosion pits compared to the steel surface under the PoPD coating. From (Figure 6) and (Figure 7), we can find that both electrochemical protection and barrier effects can protect the metal, and the electrochemical protection is reflected in the rise of the corrosion potential and the formation of the passivation layer on the surface of the metal substrate.

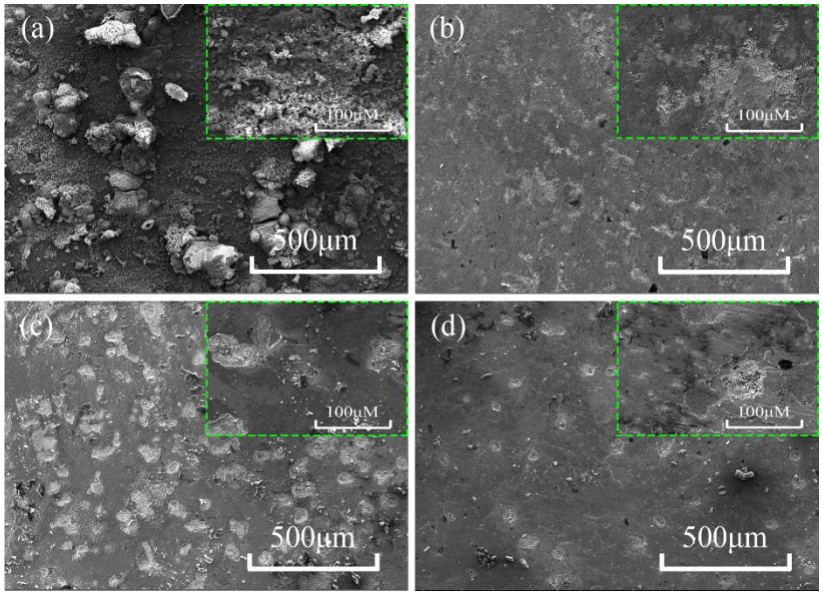

Figure 7. Stainless steel and removed coating surface (a) bare steel, (b) WPU coating, (c) PoPD coating, (d) PoPD-ZnO composite coating, which after soaked in 3.5% NaCl at room temperature solution for 30 days.

4. CONCLUSIONS

Copolymer PoPD and its polymer-nanocomposite PoPD-ZnO were successfully prepareded by chemical oxidative polymerisation. The structure and properties of the synthesized polymers are characterized by FTIR, XRD, SEM and CV. The corrosion resistance was measured by soaking in 3.5% NaCl at room temperature. The results of potentiodynamic polarization and EIS measurements show that the corrosion rates of PoPD coating and PoPD-ZnO composite coating are 0.41 and 0.05 mm/year, respectively, which is much lower than 2.57 mm/year of stainless steel base. Composite coating of PoPD-ZnO provides higher corrosion protection in 3.5% NaCl solution than WPU and copolymer PoPD coating. The SEM image after peeling off the coating showed no obvious corrosion on the steel surface under the PoPD-ZnO composite coating, indicating that when addition of nano zinc oxide is advantageous for forming a dense coating which reduces the porosity of the polymer due

to the chain structure, thereby improving the corrosion resistance of the PoPD film development.

AUTHOR CONTRIBUTIONS

All authors contributed equally to this work. Jiawei Zhang conceived the idea of the serial PoPD-ZnO material; Chaogang Zhou and Chaojin Zhou directed the experimental work and conducted the measurements. Chaogang Zhou wrote the paper. All authors participated in analyzing the experimental data and discussing the results, as well as preparing the paper.

CONFLICT OF INTERESTS

The author declares that there is no conflict of interests regarding the publication of this paper.

ACKNOWLEDGMENTS

We acknowledge financial support from Postdoctoral Daily Funds (grant no. 3103/14310335), Doctor Startup Foundation Subsidized project of North China University of Science and Technology (grant no. 28410599), The Natural Science Foundation of Hebie Province (grant no. E2018209284).

References

1. S. Pour-Ali, C. Dehghanian, A. Kosari, *Corros. Sci.*, 90 (2015) 239.
2. I. Yamaguchi, R. Morisaka, *Polym. Int*., 66 (2017) 320.
3. H. Ullah, A.A. Shah, K. Ayub, S. Bilal, *J. Phys. Chem. C*, 117 (2013) 4069.
4. G. Ebrahimi, J. Neshati, F. Rezaei, *Prog. Org. Coat.*, 105 (2017) 1.
5. S. Samanta, P. Roy, P. Kar, *Macromol. Res.*, 24 (2016) 342.
6. B. Y. Maryam, F. Lida, E. Ali, N. Maryam, *Solid State Ionics*., 324 (2018) 138.
7. M. G. Hosseini, P. Y. Sefidi, *Surf. Coat. Technol.*, 331 (2017) 66.
8. P. Sambyal, G. Ruhi, S.P. Gairola. S.K. Dhawan, B.M. Bisht, *Mater. Res. Express*, 5 (2018) 085307.
9. I.O. Arukalam, M. Meng, H. Xiao, Y. Ma, *Appl. Surf. Sci.*,433 (2018) 1113.
10. F. Zhang, H. Qian, L. Wang, Z. Wang, C. Du, X. Li, D. Zhang, *Surf. Coat. Technol.*,341 (2018) 15.
11. H. Zheng, M. Guo, Y. Shao, Y. Wang, B. Liu, G. Meng, *Corros. Sci.*, 139 (2018) 1.
12. F. Tamaddon, F. Aboee, A. Nasiri, *Catal. Commun.*, 16 (2011) 194.
13. Z. Yang, W. Zhong, C.T. Au, X. Du, H. Song, X. Qi, X. Ye, M. Xu, Y. Du, *J. Phys. Chem. C*, 113 (2009) 21269.
14. V.G. Bairi, S.E. Bourdo, N. Sacre, D. Nair, B.C. Berry, A.S. Biris, T. Viswanathan, *Sensors*, 15 (2015) 26415.
15. B. Duran, G. Bereket, M.C. Turhan, S. Virtanen, *Thin Solid Films*, 519 (2011) 5868.
16. S.M. Sayyah, M.M. El-Deeb, S.M. Kamal, R.E. Azoon, *J. Appl. Polym. Sci.*, 112 (2010) 3695.
17. P. Gajendran, R. Saraswathi, *J. Solid State Electrochem.*, 17 (2013) 2741.
18. U. Riaz, S. Jadoun, P. Kumar, M. Arish, A. Rub, S.M. Ashraf, *Acs Appl. Mater. Interfaces*, 9 (2017) 33159.
19. S. Bilal, A.U.H.A. Shah, R. Holze, *Vib. Spectrosc.*, 53 (2010) 279.
20. S. Bilal, A.U.H.A. Shah, R. Holze, *Electrochim. Acta*, 56 (2011) 3353.
21. P. Gajendran, S. Vijayanand, R. Saraswathi, *J. Electroanal. Chem.*, 601 (2007) 132.
22. L.F. D'Elia, R.L. Ortiz, O.P. Marquez, J. Marquez, Y. Martinez, *J. Electrochem. Soc.*, 148 (2001) 297.
23. A. Golgoon, M. Aliofkhazraei, M. Toorani, M.H. Moradi, A.S. Rouhaghdam, M. Asgari, *Anti-Corros. Method. M.*, 64 (2017) 380.

24. A. Ganash, *J. Nanomater.*, 2014, (2014).
25. M. Mobin, J. Aslam, R. Alam, *Arab. J. Sci. Eng.*, 42 (2016) 1.
26. N. Kannapiran, A. Muthusamy, P. Chitra, S. Anand, R. Jayaprakash, *J. Magn. Magn. Mater.*, 423 (2017) 208.
27. J. Wang, M. Wang, J. Guan, C. Wang, G. Wang, *Mater. Sci. Eng. C.*, 71 (2017) 844.
28. N. Kannapiran, A. Muthusamy, B. Renganathan; A.R. Ganesan, R. Jayaprakash, *J. Mater. Sci.*, Mater. El. 29 (2018) 3135.
29. P. Muthirulan, N. Rajendran, *Surf. Coat. Technol.*, 206 (2012) 2072.
30. S. Samanta, P. Roy, P. Kar, *Polym. Adv. Technol.*, 28 (2017) 797.
31. S. Li, C. Zhao, Y. Wang, H. Li, Y. Li, *J. Mater. Sci.*, 53 (2018) 7344.
32. P. Sambyal, G. Ruhi, H. Bhandari, S.K. Dhawanet, *Surf. Coat. Technol.*, 272 (2015) 129.
33. R. Najjar, S.A. Katourani, M.G. Hosseini, *Prog. Org. Coat.*, 124 (2018) 110.
34. M. Mobin, J. Aslam, R. Alam, *J. Adhes. Sci. Technol.*, 31 (2016) 749.
35. M.R. Mahmoudian, W.J. Basirun,; Y. Alias, A.K. Zak, *Thin Solid Films*, 520 (2011) 258.
36. S. Bilal, S. Farooq, A.A. Shah, R. Hoolze, *Synth. Met.*, 197 (2014) 144.
37. M. Selvaraj, S. Palraj, K. Maruthan, G. Rajiagopal, G. Venkatachari, *J. Appl. Polym. Sci.*, 116 (2010) 1524.